Pharmaceutical Research, Vol. 27, No. 4, April 2010 (© 2010)
DOI: 10.1007/s11095-009-0038-5

Research Paper

Formulation and *In Vitro-In Vivo* Evaluation of Black Raspberry Extract-Loaded PLGA/PLA Injectable Millicylindrical Implants for Sustained Delivery of Chemopreventive Anthocyanins

Kashappa Goud H. Desai,[1] Karl F. Olsen,[1] Susan R. Mallery,[2] Gary D. Stoner,[3] and Steven P. Schwendeman[1,4]

Received August 18, 2009; accepted December 14, 2009; published online February 11, 2010

Purpose. The objective of this study was to formulate and evaluate freeze-dried black raspberry (FBR) ethanol extract (RE) loaded poly(DL-lactic-co-glycolic acid) (PLGA) and poly(DL-lactic acid) (PLA) injectable millicylindrical implants for sustained delivery of chemopreventive FBR anthocyanins (cyanidin-3-sambubioside (CS), cyanidin-3-glucoside (CG) and cyanidin-3-rutinoside (CR)).
Methods. Identification and quantitation of CS, CG, and CR in RE was performed by mass spectroscopy and HPLC. RE:triacetyl-β-cyclodextrin (TA-β-CD) inclusion complex (IC) was prepared by a kneading method and characterized by X-ray diffraction (XRD), nuclear magnetic resonance spectroscopy (NMR) and UV-visible spectroscopy. RE or RE:TA-β-CD IC-loaded PLGA or PLA implants were prepared by a solvent extrusion method. *In vitro* and *in vivo* controlled release studies were conducted in phosphate-buffered saline Tween-80 (pH 7.4, 37°C) and after subcutaneous administration in male Sprague-Dawley rats, respectively. Anthocyanins were quantified by HPLC at 520 nm.
Results. The content of CS, CG, and CR in RE was 0.2, 1.5, and 3.5 wt%, respectively. The chemical stability of anthocyanins in solution was determined to be pH-dependent, and their degradation rate increased with an increase in pH from 2.4 to 7.4. PLGA/PLA millicylindrical implants loaded with 5 or 10 wt% RE exhibited a high initial burst and short release duration of anthocyanins (35–52 and 80–100% CG + CR release after 1 and 14 days, respectively). The cause for rapid anthocyanins release was linked to higher polymer water uptake and porosity associated with the high osmolytic components of large non-anthocyanin fraction of RE. XRD, ^{1}H NMR and UV-visible spectroscopy indicated that the non-anthocyanin fraction molecules of RE formed an IC with TA-β-CD, decreasing the hydrophilicity of RE. Formation of an IC with hydrophobic carrier, TA-β-CD, provided better *in vitro/in vivo* sustained release of FBR anthocyanins (16–24 and 97–99% CG + CR release, respectively, after 1 and 28 days from 20 wt% RE:TA-β-CD IC/PLA implants) over 1 month, owing to reduced polymer water uptake and porosity.
Conclusion. PLA injectable millicylindrical implants loaded with RE:TA-β-CD IC are optimal dosage forms for 1-month slow and continuous delivery of chemopreventive FBR anthocyanins.

KEY WORDS: black raspberry anthocyanins; chemoprevention; controlled release; inclusion complex; injectable millicylindrical implants; microencapsulation; oral cancer; PLA; PLGA; Triacetyl-β-cyclodextrin.

INTRODUCTION

The American Cancer Society estimates that over 35,000 Americans will be diagnosed with oropharyngeal cancer in 2009 (1). Due to the aggressive nature of the disease, the potential for local tumor recurrence and the possibility for development of a second primary cancer, 5-year survival rates for patients with oral squamous cell carcinoma (oral SCC) remain among the lowest of solid tumors (2–4). Cancer chemoprevention, which entails the use of naturally or synthetically derived substances to prevent, inhibit or reverse malignant transformation, could positively impact oral SCC outcomes in two respects. First, chemoprevention could prevent progression of the recognized premalignant lesions of oral epithelial dysplasia to overt oral SCC. Secondly, for persons with previously treated oral SCC, chemoprevention could inhibit local tumor recurrence or development of a new, second primary tumor (5). As numerous complex molecular and biochemical perturbations accompany oral cancer development, current strategies for oral cancer chemoprevention propose use of cocktails comprised of agents with complementary mechanisms of action instead of reliance on a single agent.

[1] Department of Pharmaceutical Sciences, University of Michigan, 428 Church St., Ann Arbor, USA.
[2] Department of Oral Maxillofacial Surgery and Pathology, College of Dentistry and the Comprehensive Cancer Center and Solove Research Institute, The Ohio State University, Columbus, Ohio, USA.
[3] Department of Internal Medicine, College of Medicine and the Comprehensive Cancer Center and Solove Research Institute, The Ohio State University, Columbus, Ohio, USA.
[4] To whom correspondence should be addressed. (e-mail: schwende@umich.edu)

Previously, we demonstrated that glutathione and N-acetylcysteine inhibit activation and function of an enzyme that enables progression of oral epithelial dysplasia to invasive oral SCC, i.e. matrix metalloproteinase-9 (6). In light of the potential for oral cancer chemopreventive applications, we subsequently formulated and characterized PLGA implants capable of sustained release of N-acetylcysteine (5). Additional, natural-product-focused studies from our labs showed that freeze-dried black raspberries possess chemopreventive properties that are potentially additive or complementary to those provided by NAC (6–10).

The black raspberry (*Rubus occidentalis*), a perennial shrub native to North America, contains many compounds with potential chemopreventive effects, including anthocyanins (cyanidin-3-glucoside (CG), cyanidin-3-sambubioside (CS), cyanidin-3-rutinoside (CR), cyanidin-3-xylosylrutinoside, and pelargonidin-3-rutinoside) (8,11), phenolics (ellagic, ferulic, and *p*-coumeric acid), vitamins (ascorbic acid, α and β-carotene and folate), and minerals (12). Studies from our labs have shown that freeze-dried black raspberry (FBR) ethanol extract (RE) possesses cancer-preventing properties at both the *in vitro* and *in vivo* levels (6–10,13). Importantly, no deleterious effects were observed in any of our Phase I human clinical trials of FBR (13–15). Additional studies have shown that the anthocyanin-enriched fraction is the FBR component responsible for inhibition of tobacco-associated carcinogen, redox-mediated activation of the pleiotropic transcription activating factors NF-κB and AP-1 (16–18). Recent *in vivo* studies have confirmed that anthocyanin-rich extracts are the major FBR components responsible for prevention of esophageal tumors in a rodent model (18). The non-anthocyanin FBR fraction, however, may also contribute to FBR's chemopreventive effects. Non-anthocyanin fraction molecules (phenolics, vitamins, and minerals) of FBR were found to influence the chemopreventive potential of anthocyanins (12,13), signifying the necessity of this fraction in controlled release formulations. Topical application of 10 wt% FBR gel to oral premalignant lesions resulted in positive therapeutic effects, including reduction in histologic grade, decrease in loss of heterozygosity at tumor suppressor gene associated loci, and significant reduction in lesional epithelial cyclooxygenase-2 levels (6,9,10,13). Based on these preliminary *in vitro-in vivo* results (6,9,10,13), we formulated and characterized RE-loaded PLGA/PLA millicylindrical implants in the current study for long-term localized delivery of FBR anthocyanins.

Implantable poly(DL-lactic-co-glycolic acid) (PLGA) and poly(DL-lactic acid) (PLA) vehicles have been well-demonstrated as potential vehicles for maintaining local tissue levels of therapeutic agents for extended time periods (19–21). In addition to their ability to provide therapeutically relevant local levels without systemic effects, PLGA implants provide another significant clinical benefit. Unlike standard local delivery formulations (gel, cream and ointment for example), which require multiple, repeated dosing throughout the day, PLGA/PLA implantable vehicles alleviate concerns with multiple dosing schedules and poor patient compliance (19–21).

In this study, PLGA and PLA injectable millicylindrical implants were selected for development of controlled release anthocyanins (CS, CG, and CR) in oral SCC. First, identification and determination of the relative amount of anthocyanins in RE were performed by mass spectroscopy and HPLC. The chemical stability of FBR anthocyanins in the medium used for the release study and the effect of pH on their chemical stability was then investigated. Finally, the ability of formulation strategies, such as RE loading, polymer hydrophobicity (lactide:glycolide ratio) and formation of hydrophobic inclusion complex (IC) of RE molecules with triacetyl-β-cyclodextrin (TA-β-CD) to provide slow and continuous *in vitro*/*in vivo* release of anthocyanins, was thoroughly investigated. RE:TA-β-CD inclusion complex (RE:TA-β-CD IC) was characterized by XRD, NMR, and UV-visible spectroscopy.

MATERIALS AND METHODS

Materials

Reference CS was purchased from Polyphenols Laboratories (Sandnes, Norway). Reference CG and CR were purchased from Indofine Chemical Company, Inc. (Hillsborough, NJ, USA). PLGA 50:50 (inherent viscosity, i.v. = 0.57 dl/g and weight average molecular weight, M_w = 51 kDa), PLGA 85:15 (i.v. = 0.61 dl/g and M_w = 95 kDa) and PLA (i.v. = 0.58 dl/g and M_w = 84.5 kDa) were purchased from Medisorb, Alkermes Inc. (Cambridge, MA, USA). All polymers used were lauryl ester end-capped. NMR (5 mm) tubes, phosphoric acid-d_3 (D_3PO_4), deuterium oxide, ethanol-d_6, Tween® 80 and TA-β-CD were purchased from Sigma-Aldrich Chemical Co. (St. Louis, MO, USA). Xylazine (AnaSed®) injection was purchased from LLoyd Laboratories (Shenandoah, Iowa, USA). Ketamine hydrochloride (Ketaset) injection was purchased from Fort Dodge Animal Health (Fort Dodge, Iowa, USA). All other chemicals, reagents and solvents (analytical or purer grade) were purchased from commercial suppliers.

Black raspberries (*Rubus occidentalis*) were obtained from a single farmer each year (Stokes Fruit Farm, Wilmington, OH, USA). They are of the same variety (Jewel), grown in the same part of the field, and picked at about the same degree of ripeness (when the majority of the berries in a cluster have turned black—this occurs within a period of 1–2 weeks). The berries are harvested mechanically (with a picker) in a total period of 4 h. During the picking process, the berries are washed mechanically, and each batch is frozen at −20°C within 1 h of the time of harvest. The variation in CS, CG and CR content in black raspberries picked over a period of 5 years was determined to be 10–20 wt%. For the current study, the ethanol extract of freeze-dried black raspberries (RE) was obtained as described previously (8).

Mass Spectroscopy

Full scan mass spectroscopic data were acquired in the positive mode from m/z 100–700 by using a mass spectrometer (AutoSpec Ultima, Micromass/Waters Corporation, Milford, MA, USA). The ESI voltage, capillary temperature,

sheath gas pressure, and auxiliary gas were set at 39 V, 300°C, 65 psi, and 20 psi, respectively.

Anthocyanin HPLC Assay

All HPLC assays were performed on a Waters 2695 *alliance* system (Milford, MA, USA) consisting of a 2996 Photodiode array (PDA) detector and a personal computer with Empower 2 Software. An Econosphere C18 (4.6 × 250 mm) reverse phase column (Alltech, USA) was used at a flow rate of 1.0 mL/min. Separation of the CS, CG, and CR was achieved using the following mobile phases: (A) 1.5% (*v*/*v*) phosphoric acid and (B) formic acid: acetonitrile: phosphoric acid:water (20:26:1.5:52.5). The solvent gradient was as follows: initial composition 80% A and 20% B, changing to 30% A and 70% B at 25 min, then 10% A and 90% B at 30 min and held until 35 min. Finally, the composition returned to 80% A and 20% B (initial conditions) at 40 min before another sample injection at 45 min. All gradient curves were linear. The sample injection volume was 20 μL, and the detection wavelength was 520 nm. Chromatography data were collected and processed using an Empower PDA Software. Standard curves of reference compounds (CS, CG, and CR) were established in 1.5% (*v*/*v*) phosphoric acid solution and concentration of CS, CG, and CR in unknown samples was calculated from their respective standard curve.

Chemical Stability of FBR Anthocyanins

Chemical stability of anthocyanins (CS, CG, and CR) was studied in two steps. First, chromatographic and visible spectroscopic characteristics of degradation products of anthocyanins were obtained by studying the degradation of each reference compound at a concentration = 18 μg/mL in phosphate-buffered saline Tween-80 (PBST) (pH 7.4). Then, using the 0.1 mg/mL RE, the degradation profile of CS, CG, and CR in PBST and effect of pH (2.4, 5.0 and 7.0) on the anthocyanin (CR) degradation rate was studied. All the solutions were taken into separate 1-mL amber-colored ampoules and sealed under vacuum. Ampoules were placed in an incubator maintained at 37°C and shaken at 100 RPM. At predetermined time intervals, three ampoules were taken out and fraction of remaining anthocyanins was determined by HPLC.

Preparation of RE:TA-β-CD IC

RE:TA-β-CD IC was prepared by a kneading method. Briefly, the required amounts of RE and TA-β-CD (1:1 mass ratio) were triturated with a small amount of 80/20 ethanol/1.5% (*v*/*v*) phosphoric acid solution and kneaded thoroughly for 1 h. The resulting slurry was dried under vacuum at room temperature for 24 h and passed through a stainless steel sieve to obtain the particle size of <90 μm.

X-ray Diffraction (XRD)

The XRD pattern of RE, TA-β-CD and RE:TA-β-CD IC was obtained using a Scintag powder X-ray diffractometer (Scintag Inc., Cupertino, CA, USA). The X-ray source was copper Kα (40 kV, 30 mA), and the scanning speed was 3 deg/min.

Nuclear Magnetic Resonance Spectroscopy (NMR)

About 1 mg/mL RE or TA-β-CD or RE:TA-β-CD IC samples were prepared by dissolving the required amount in 1.5% (*v*/*v*) D_3PO_4 for RE or 80/20 (*v*/*v*) CD_3CD_2OD/1.5% (*v*/*v*) D_3PO_4 for TA-β-CD and RE:TA-β-CD IC. About 1 mL of RE, TA-β-CD and RE:TA-β-CD IC solutions were transferred into 5 mm NMR tubes, and one-dimensional ^1H NMR spectra were recorded on a Bruker Avance DRX-500 spectrometer (Bruker BioSpin Corporation., Billerica, MA, USA). Typical acquisition parameters consisted of 64 K points covering a sweep width of 10330 Hz, a pulse width (pw90) of 11 μs, and a 0.5 Hz exponential function was applied to the FID before Fourier transformation. The resonances due to residual solvents (water, phosphoric acid and ethanol), present as impurities, were used as internal reference.

UV-Visible Spectroscopy

Stock solutions of RE (1 mg/mL) and TA-β-CD (10 mg/mL) were prepared in 80/20 ethanol/1.5% (*v*/*v*) phosphoric acid solution. At a fixed RE concentration (0.1 mg/mL), solutions of RE/TA-β-CD with varying amount of TA-β-CD (0, 1, 2, 4, 8, and 9 mg/mL) were then prepared. All the solutions in amber-colored vials with screw-caps were incubated at room temperature for 1 h with constant agitation, and then UV-visible spectra were obtained on a UV-visible spectrophotometer (Beckman Instruments Inc., Fullerton, CA, USA).

Preparation of RE/PLGA, RE/PLA and RE:TA-β-CD IC/PLA Millicylindrical Implants

RE or RE:TA-β-CD IC-loaded millicylindrical implants were prepared by the solvent extrusion method as described previously (5). Briefly, PLGA or PLA was dissolved in acetone to make a final polymer concentration of 55% (w/w) with respect to solvent weight. Sieved (<90 μm) RE (5 and 10 wt%) or RE:TA-β-CD IC (20 wt%) was added to polymer solution to form RE or RE:TA-β-CD IC/polymer mixture. The mixtures were loaded into a 3-ml syringe and slowly extruded into the silicone tubing (I.D = 0.8 mm). The solvent-extruded product was dried at room temperature for 48 h and then in a vacuum oven at 40°C for another 72 h before testing.

Determination of Anthocyanin Loading

To determine the relative amount of CS, CG and CR in RE, ~1 mg RE (n=3) was dissolved in 1.5% (*v*/*v*) phosphoric acid solution, injected into the HPLC system and concentration was determined using the calibration curve of respective reference compound. Then, the theoretical loadings of CS, CG and CR in 5 and 10 wt% RE or 20 wt% RE:TA-β-CD IC-loaded implants were calculated. To determine the actual loadings of CS, CG and CR in RE or RE:TA-β-CD

IC-loaded implants, ~6 mg implants (n=3) were placed in 5 ml glass vials. To these vials, 2 mL methylene chloride and 1 mL of 1.5% (v/v) phosphoric acid solution were added, followed by spinning for 5 min. The phosphoric acid solution layer was taken out, injected into the HPLC system, and concentration of CS, CG and CR was determined using the calibration curve of respective reference compound. CS, CG and CR loading was calculated as the percentage of amount of CS or CG or CR *versus* the total weight of mixture (i.e., RE or RE:TA-β-CD IC and PLGA/PLA).

Evaluation of *In Vitro* Anthocyanin Release from RE/PLGA, RE/PLA and RE:TA-β-CD IC/PLA Millicylindrical Implants

In vitro release studies were conducted in PBST (pH 7.4) under perfect sink conditions. About 5 mg of RE or RE:TA-β-CD IC-containing millicylinders were weighed and placed in 1-ml amber-colored ampoules (3 ampoules for each sampling interval). Exactly 1 ml PBST was added to all ampoules and sealed under vacuum. The ampoules were placed in an incubator maintained at 37°C and shaken at 100 RPM. At predetermined time intervals (1, 3, 7, 14, 21, and 28 days), three ampoules were taken out and broken, and implants were freeze-dried immediately. The amount of anthocyanins remaining in each implant was determined similarly as described in loading determination. The cumulative amount of released anthocyanins was determined by subtracting the content remaining in the implants from the initial loading.

Evaluation of *In Vivo* Anthocyanin Release from RE: TA-β-CD IC/PLA Millicylindrical Implants

The treatment of experimental animals was in accordance with University of Michigan animal care guidelines, and all NIH guidelines for the care and use of laboratory animals were observed. Male Sprague-Dawley rats of 7–8 weeks old (weighing 250–300 g) were housed in cages and given free access to standard laboratory food and water. Animals were anesthetized with a 9:1 mixture of ketamine (100 mg/ml) and xylazine (100 mg/ml) administered by intraperitoneal injection of 0.5–1.0 mL/kg body weight. RE:TA-β-CD IC/PLA millicylindrical implants (length = ~1 cm and weight = ~7 mg) were subcutaneously implanted into the dorsal region of rats. At different implantation duration (1, 7, 14, 21, and 28 days), the rats were euthanized, and implants (n=5) were carefully recovered by removing the skin. The tissue adhered to the implants was carefully removed with the help of forceps, and then the implants were freeze-dried. The amount of anthocyanins remaining in each implant was determined similarly as described in loading determination. The cumulative *in vivo* anthocyanins release was determined by subtracting the content remaining in the implants from the initial loading.

Measurement of *In Vitro-In Vivo* Water Uptake of PLGA/PLA Implants

After 1, 3, 7, 14, 21, and 28 days of incubation in PBST (pH 7.4) or subcutaneous implantation in male Sprague-Dawley rats (see *in vivo* anthocyanin release study section for subcutaneous implantation and recovery procedure), implants were blotted with tissue paper, weighed immediately, and then freeze-dried. Freeze-dried implants were weighed again, and water content of the implant was calculated by

$$\text{Water uptake } (\%) = \frac{W_1 - W_2}{W_2} \times 100 \qquad (1)$$

where W_1 and W_2 are the weights of the wet and dry implants, respectively.

Scanning Electron Microscopy

The inner morphology of RE and RE:TA-β-CD IC-loaded implants was examined using a Hitachi S3200N scanning electron microscope (Hitachi Ltd., Tokyo, Japan). The millicylinders were fixed previously on a brass stub using double-sided adhesive tape and then were made electrically conductive by coating, in a vacuum, with a thin layer of gold (approximately 3 to 5 nm) for 60 s at 40 W. The cross-sectional

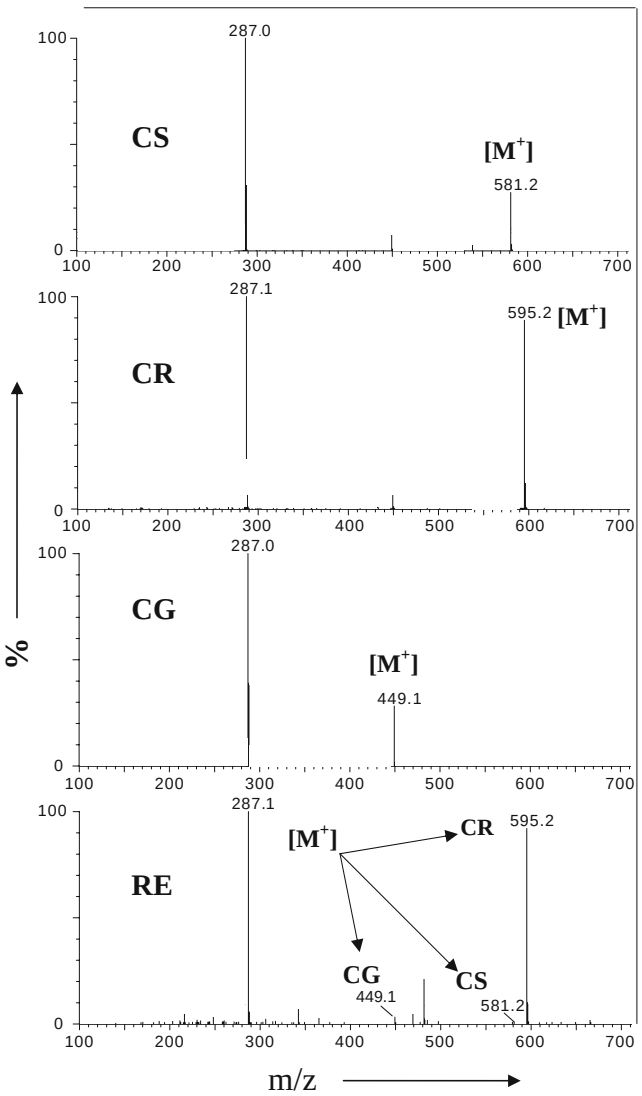

Fig. 1. Identification of anthocyanins in RE. Mass spectrum of RE and reference CS, CG and CR. M^+: molecular ion peak.

Table I. Chromatographic, Visible Spectroscopic, Mass Spectral and Relative Abundance Data of FBR Anthocyanins

FBR Anthocyanin	λ_{max} (nm)	HPLC (t_R) (min)	Molecular ion (Da)	Fragment ion (Cyanidin) (Da)	Theoretical M_w (Da)[b]	Relative Quantity (wt%)[a]
CS	520	17.3	581.2	287	581.0	0.23±0.01
CG	520	17.8	449.1	287	449.2	1.53±0.04
CR	520	18.8	595.2	287	595.0	3.53±0.06

[a] Mean ± SE, n=3
[b] Based on reference 24
CS: Cyanidin-3-Sambubioside; *CG*: Cyanidin-3-Glucoside; *CR*: Cyanidin-3-Rutinoside

view images of millicylinders were taken at an excitation voltage of 20 kV.

RESULTS AND DISCUSSION

Identification and Quantitation of Anthocyanins in RE

Anthocyanins are a group of flavonoids responsible for the red, violet, and blue colors of most of berries and fruits. Berries have been identified as one of the richest sources of anthocyanins. Among the berries, black raspberries (*Rubus occidentalis*) were found to contain the highest amount of anthocyanins (11,22,23). Cyanidin is one of the six most commonly found anthocyanin aglycones (pelargonidin, cyanidin, peonidin, delphinidin, pentunidin, and malvidin). Different types and numbers of sugars (e.g., glucose, rhamnose, xylose) conjugated to the cyanidin form numerous structures of anthocyanins (e.g., CG, CS, and CR). (8,11,13,22,23).

In the present study, the identification and quantitation of chemopreventive anthocyanins in RE was performed by mass spectroscopy and HPLC. In mass spectroscopy, the mass spectra of RE and reference compounds (CS, CG, and CR) were obtained (see Fig. 1). CS, CG, and CR in RE were identified by comparing the molecular masses (M^+) of reference compounds with those of RE sample (see Table I). As shown in Fig. 1, the mass spectrum of all the three reference compounds showed the precursor peak at m/z

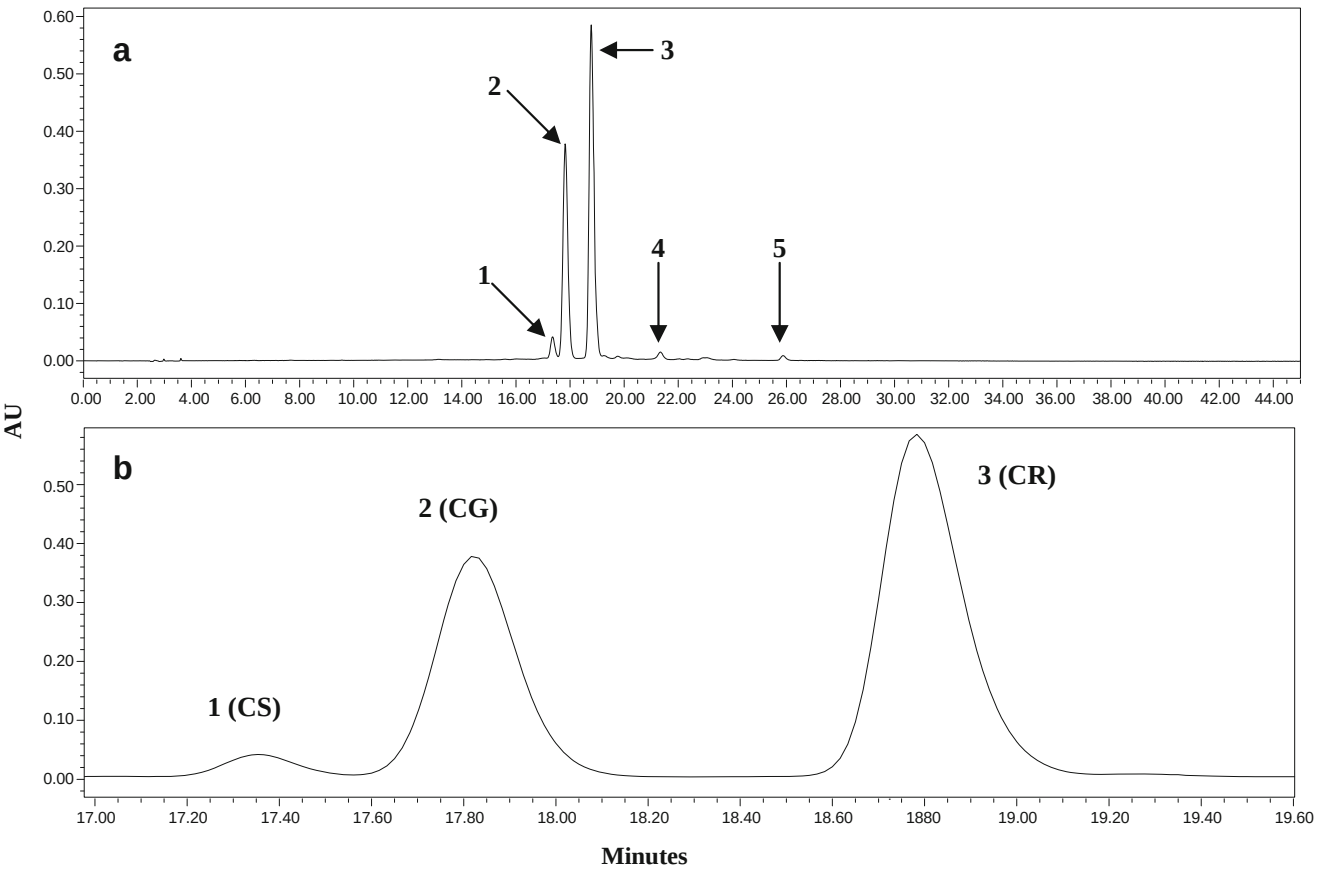

Fig. 2. Identification and determination of elution profiles of anthocyanins (CS, CG and CR) by HPLC with detection at 520 nm. **a:** A typical HPLC profile of RE (1 mg/mL in 1.5% (*v*/*v*) phosphoric acid solution). **b:** Chromatogram of CS, CG and CR.

Table II. Chromatographic and UV Spectroscopic Data of Degradation Products of FBR Anthocyanins

Degradation product	HPLC (t_R) (min)			λ_{max} (nm)		
	CS	CG	CR	CS	CG	CR
I	12.4	12.8	12.4	340	344	351
II	6.6	6.4	6.2	293	294	292
III	5.3	5.2	5.0	288	285	287

CS: Cyanidin-3-Sambubioside; *CG*: Cyanidin-3-Glucoside; *CR*: Cyanidin-3-Rutinoside

287 corresponding to cyanidin. Ions at *m/z* 581.2, 449.1, and 595.2 in reference compound samples corresponded to the molecular cations (M^+) of CS, CG, and CR, respectively. Mass spectrum of RE also showed the peaks at *m/z* 581.2 (CS), 449.1 (CG), and 595.2 (CR) along with the precursor (cyanidin) peak at *m/z* 287, indicating the presence of three chemopreventive anthocyanins of black raspberry (8,12,13) in the encapsulated extract. Further, the molecular weight (M_w) of anthocyanins identified in RE corresponded with their theoretical M_w (24) (see Table I). MS/MS fragmentation data obtained with RE and reference compound samples was consistent with the anthocyanins structures (8,11,13,22,23). Loss of M^+−294.1, M^+−162, and M^+−308.1 respectively from CS, CG, and CR molecules corresponded to the cleavage of sambubiosyl, glucosyl, and rutinosyl units, respectively. The current identifications are consistent with the previously published information on black raspberry anthocyanins (8,11,13,22,23).

Further, identification and determination of elution profile and relative abundance of anthocyanins in RE were performed by the chromatographic techniques (see Fig. 2). A typical HPLC profile (see Fig. 2a) displayed 5 peaks at a detection wavelength of 520 nm, obtained from 1 mg/mL RE in 1.5% (*v/v*) phosphoric acid. All the peaks in chromatogram are well-separated, suggesting the effectiveness of the HPLC method. The peak corresponding to CS, CG, and CR was identified by co-elution. A known amount of reference compounds (CS, CG and CR) was separately dissolved in 1-mL RE solution (1 mg/mL in 1.5% (*v/v*) phosphoric acid) and injected into the HPLC system. The peak (1–5) area obtained

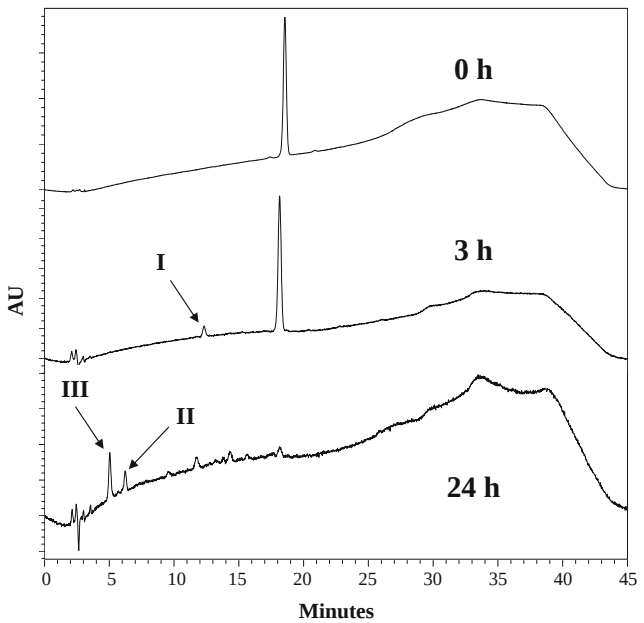

Fig. 3. Identification and determination of elution profile of degradation products of reference CR by HPLC. HPLC chromatograms of CR solution (concentration = 18 μg/mL in PBST (pH 7.4)) at 0, 3, and 24 h of incubation at 37°C. Peaks I, II, and III are degradation products of CR in the order of formation.

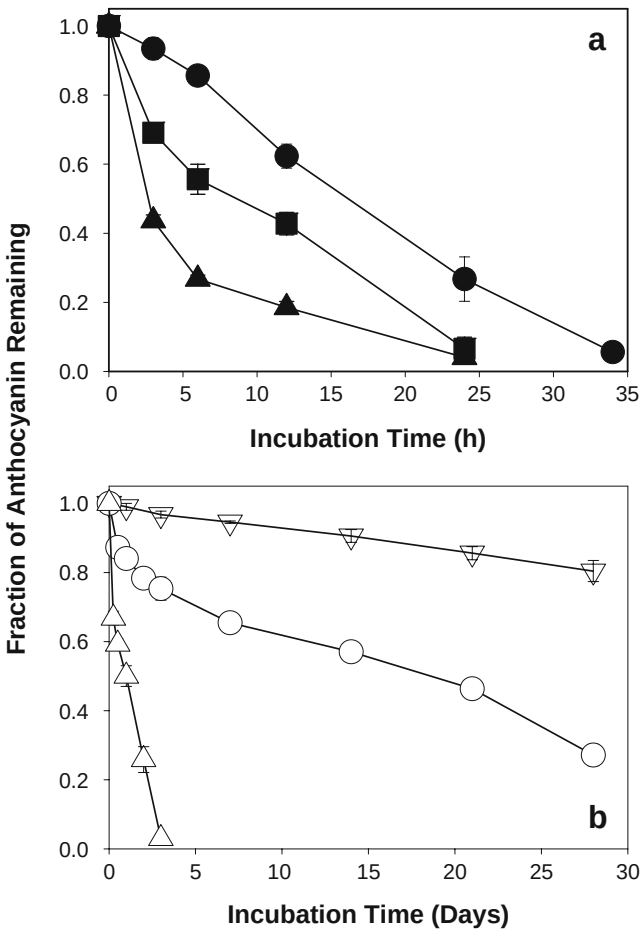

Fig. 4. Chemical stability of RE anthocyanins (CS, CG and CR). **a**: Relative degradation profile of CS (*filled square*), CG (*filled circle*) and CR (*filled triangle*) in the medium used for release study (PBST (pH = 7.4)). **b**: Effect of pH (2.4 (*open inverted triangle*), 5.0 (*open circle*), and 7.0 (*open triangle*)) on the degradation rate of a highly unstable anthocyanin (CR). All the RE (0.1 mg/mL in PBST (***a***) or buffers (***b***)) solutions in sealed amber-colored ampoules were incubated at 37°C. Symbols represent mean ± SE (n=3).

Table III. Evaluation of the Microencapsulation of FBR Anthocyanins (Cyanidin-3-Sambubioside (CS), Cyanidin-3- Glucoside (CG) and Cyanidin-3- Rutinoside (CR)) in Millicylindrical PLGA and PLA Implants

Millicylindrical formulation	Polymer	Theoretical loading (%w/w)					Loading efficiency(%)[a]			
		RE	CS	CG	CR	Total Anthocyanins (CS + CG + CR)	CS	CG	CR	Total Anthocyanins (CS + CG + CR)
RE	PLGA 50:50 (i.v = 0.57 dl/g and M_w = 51 kDa)	5.00	0.012	0.081	0.16	0.256	78.7 ± 1.9	79.5±7.5	79.7±5.5	81.6±6.1
	PLGA 50:50 (i.v = 0.57 dl/g and M_w = 51 kDa)	10.1	0.025	0.17	0.35	0.545	80.7±3.5	89.8 ± 2.7	91.1 ± 3.8	90.2 ± 2.8
	PLGA 85:15 (i.v = 0.61 dl/g and M_w = 95 kDa)	10.1	0.025	0.17	0.35	0.545	78.6 ± 2.6	87.3±4.2	92.0±4.3	90.3±4.1
	PLA 100DL (i.v = 0.58 dl/g and M_w = 84.5 kDa)	10.1	0.025	0.17	0.35	0.545	89.6 ± 1.9	93.8±3.2	92.3±3.3	93.0 ± 2.7
RE:TA-β-CD IC	PLA 100DL (i.v = 0.58 dl/g and M_w = 84.5 kDa)	10.6	0.026	0.18	0.36	0.574	90.3±3.0	94.6±4.1	93.5 ± 2.2	93.2 ± 1.5

[a] Mean ± SE, $n=3$

RE: freeze-dried black raspberry extract, *PLA*: poly(lactic acid), *PLGA*: poly(DL-lactide-co-glycolide), *TA-β-CD*: triacetyl-β-cyclodextrin; *RE*:TA-β-CD IC: *RE*:TA-β-CD inclusion complex

by RE (1 mg/mL) and RE (1 mg/mL) + reference compounds solutions were compared to identify each anthocyanin. Peaks 1, 2, and 3 in Fig. 2b were respectively identified as CS, CG, and CR, as co-injection of the respective reference compound led to an increase in area (*data not shown*) of peaks 1, 2, and 3, respectively. CS, CG, and CR exhibited a maximum UV absorption at 520 nm and eluted at the retention time of 17.3, 17.8 and 18.8 min, respectively (see Table I). To determine the relative amount of CS, CG, and CR in RE, about 1 mg ($n=3$) RE was dissolved in 1.5% (*v*/*v*) phosphoric acid solution and analyzed by HPLC. The relative abundance of CS, CG, and CR in RE was 0.23, 1.53, and 3.53 wt%, respectively (see Table I).

Chemical Stability of FBR Anthocyanin

Identification of Degradation Products of CS, CG, and CR

The chromatographic and UV spectroscopic characteristics of degradation products of CS, CG, and CR were first obtained using respective reference compounds by HPLC (with PDA detector) analysis. Reference compound solutions

Fig. 5. Effect of RE loading (theoretical) on cumulative anthocyanin (sum of CG and CR) release (**a**) and polymer water uptake (**b**) characteristics of PLGA 50:50 (i.v = 0.57 dl/g) implants millicylindrical implants. Polymer water uptake characteristics of blank (*filled reverse triangle*) and cumulative anthocyanin release and polymer water uptake characteristics of 5 (*filled circle*) and 10 (*open circle*) wt% RE-loaded implants. Studies were carried out in PBST (pH 7.4) at 37°C and symbols represent mean ± SE, $n=3$.

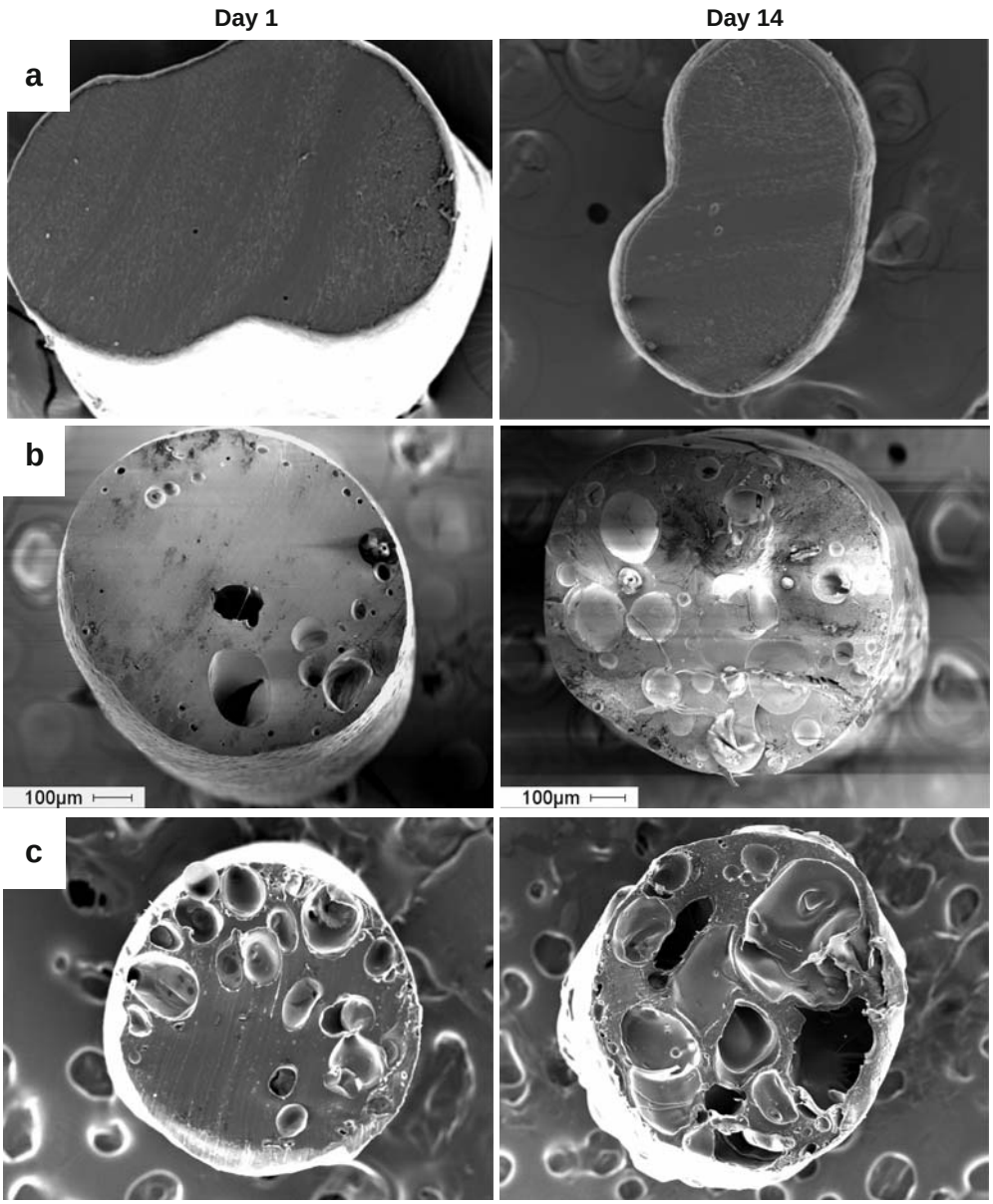

Fig. 6. Effect of RE loading (theoretical) on inner morphology of PLGA 50:50 (i.v = 0.57 dl/g) millicylindrical implants after 1 and 14 days of immersion in PBST at 37°C. SEM images are displayed for 0 (**a**), 5 (**b**), and 10 (**c**) wt% RE-loaded PLGA 50:50 millicylindrical implants.

(CS, CG, and CR) were separately prepared in PBST (pH 7.4), incubated at 37°C over a period of 34 h and analyzed. During this interval, each reference compound showed 3 new chromatographic peaks, suggestive of degradation products. The chromatographic and UV spectroscopic data of degradation products for each reference compound are presented in Table II. Degradation products were assigned product I, II, and III in the order of appearance in the HPLC chromatogram during the study period. Further, degradation products (I, II and III) of all the three reference compounds (CS, CG, and CR) exhibited a close relationship, indicating a close structural similarity. The chromatographic characteristics of degradation products of reference compounds were used to identify the degradation products of RE's anthocyanins in release study polymer samples. Since all the three reference compounds exhibited the same chromatographic pattern, the chromatograms of one reference compound (CR) solution at different time points is shown in Fig. 3.

Degradation Rate of FBR Anthocyanins and Effect of pH

The stability of black raspberry anthocyanins is highly dependent on pH and presence of other ingredients (13,25–27). Hence, the degradation profiles of FBR anthocyanins in the medium used for release study (PBST) (pH 7.4) and effect of pH on the stability of the RE anthocyanin CR was studied and displayed in Fig. 4. As shown in Fig. 4a, CR exhibited the fastest degradation (81 and 96% degradation after 12 and 24 h of incubation, respectively) over a period of 24 h, whereas CG exhibited slowest degradation (38 and 94%

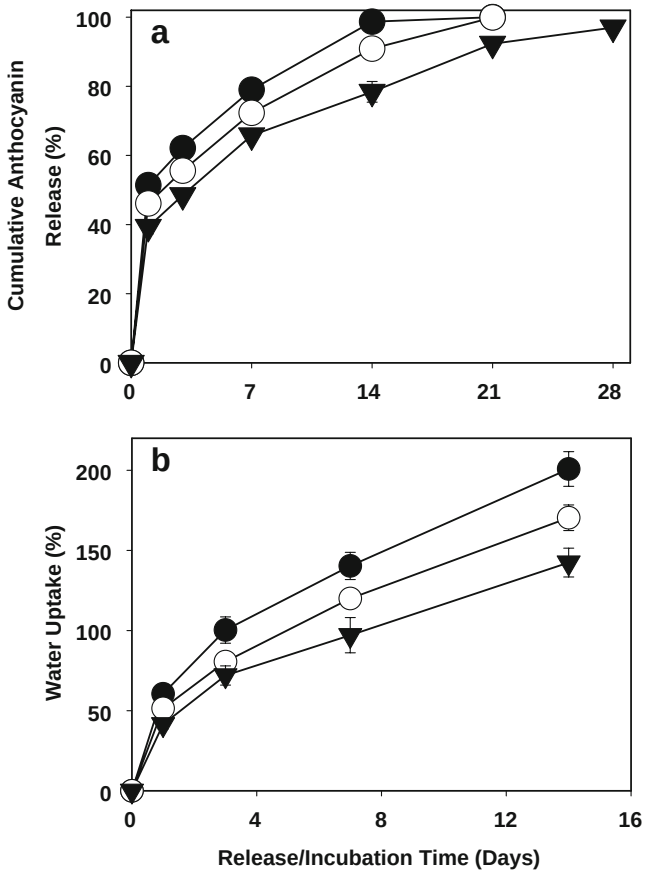

Fig. 7. Effect of polymer lactide content on cumulative anthocyanin (sum of CG and CR) release (**a**) and polymer water uptake (**b**) characteristics of millicylindrical implants. Lactide:glycolide ratio was varied from 50:50 (*filled circle*), 85:15 (open circle), and 100:0 (*filled reverse triangle*). RE loading (theoretical) in all formulations was 10 wt%, and studies were carried out in PBST (pH 7.4) at 37°C. Inherent viscosity of PLGA 50:50, PLGA 85:15, and PLA polymer was 0.57, 0.61, and 0.58 dl/g, respectively. Symbols represent mean ± SE, $n=3$.

degradation after 12 and 34 h of incubation, respectively), and intermediate degradation rate was observed with CS (57 and 93% degradation after 12 and 24 h of incubation, respectively). To understand the effect of acidic to neutral pH on the stability of FBR anthocyanins, we then investigated the stability of CR at three different pH values (2.4, 5.0 and 7.0). The effect of pH on the stability profile of CR at 37°C is displayed in Fig. 4b. At highly acidic pH 2.4, the CR degradation rate was very slow, with 80% CR remaining after 28 days. At neutral pH, complete degradation of CR occurred in 3 days. Intermediate degradation rate was observed at pH 5.0 (27% CR remaining after 28 days).

Optimization of Millicylindrical Implant Formulation Parameters with PLGA and PLA Polymers for Sustained Release of FBR Anthocyanins

Anthocyanin Loading Efficiencies of PLGA and PLA Millicylindrical Implants

Because of their potential oral SCC chemopreventive properties, there is an increasing implication to develop vehicles for localized controlled delivery of FBR anthocyanins (8,12–14,28–30). Implantable polymeric vehicles, particularly injectable configuration (e.g., millicylindrical), are the potential carriers to tune the release locally, because of the ability to control the loading and migration of the implant (20,21,31). RE or RE:TA-β-CD IC-loaded millicylindrical PLGA and PLA implants were prepared by a solvent extrusion method. Three FBR anthocyanins (CS, CG, and CR) were identified in encapsulated RE. We evaluated the loading efficiency of each and total anthocyanins in the implants. As shown in Table III, in each formulation, the loading efficiency of each and total anthocyanins in PLGA and PLA implants was very high (79–95%), suggesting the effectiveness of anthocyanins loading by a solvent extrusion method.

Effect of RE Loading on In-Vitro Anthocyanin Release from PLGA 50:50 Implants

All the anthocyanins degraded completely within 40 h of incubation in PBST (pH 7.4) at 37°C. We evaluated the *in vitro* anthocyanin release by determining the remaining amount in the implants. In an effort to optimize the controlled release millicylindrical implant formulation parameters, we first prepared the PLGA 50:50 implants loaded with 5 and 10 wt% RE (theoretical) and evaluated the release profiles. Among the three anthocyanins, the amount of CS remaining in the polymer rapidly fell below the detection limit, and hence it was not possible to obtain an accurate release profile of CS. The effects of RE loading on sum of anthocyanins (CG + CR) release and polymer water uptake profiles of PLGA 50:50 millicylindrical implants are shown in Fig. 5. As shown in Fig. 5a, implants with 5 and 10 wt% RE exhibited high initial burst and short release duration of anthocyanins (39–52 and 89–99% CG + CR release after 1 and 14 days, respectively). Implants with 5 and 10 wt% RE exhibited high polymer water uptake (see Fig. 5b) and highly porous polymer matrices (see Fig. 6) compared to blank implants, suggesting very rapid release of RE molecules from the PLGA 50:50 implants, leading to high initial burst and short release duration of anthocyanins. On the other hand, there was no significant difference in release between individual anthocyanins (*data not shown*).

Effect of Polymer Lactide/Glycolide Ratio on In-Vitro Release of Anthocyanins

In an effort to reduce the high initial burst effect and short release duration of anthocyanins, we used polymers with higher lactide content (PLGA 85:15 and PLA) to prepare 10 wt% RE-loaded implants. The effect of lactide: glycolide ratio on sum of anthocyanins (CG + CR) release and polymer water uptake profiles of millicylindrical implants are shown in Fig. 7. As the lactide content increased in the polymer, the implants exhibited slightly reduced initial burst and improved prolonged release duration of anthocyanins (see Fig. 7a). Consistent with the anthocyanin release behavior, lower polymer water uptake (see Fig. 7b) and porosity (see Fig. 8) were exhibited by the higher lactide content polymer implants. Further, we found no difference in

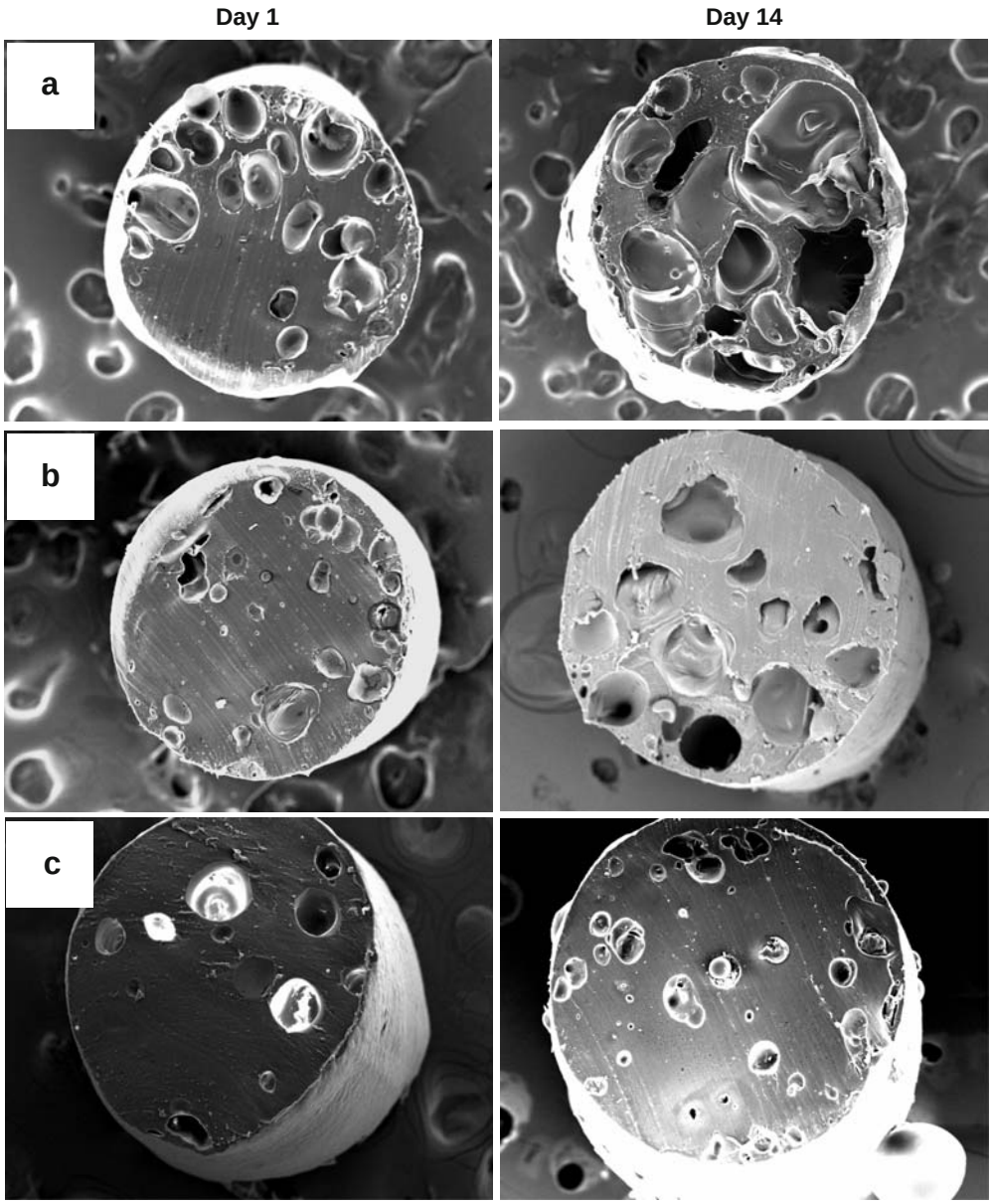

Fig. 8. Effect of polymer lactide content (50–100%) on inner morphology of millicylindrical implants after 1 and 14 days of immersion in PBST at 37°C. SEM images are displayed for 10 wt% (theoretical) RE-loaded PLGA 50:50 (i.v. = 0.57 dl/g) (**a**), PLGA 85:15 (i.v. = 0.61 dl/g) (**b**), and PLA (i.v. = 0.61 dl/g) (**c**) implants.

release between individual anthocyanins from higher lactide content polymer implants (*data not shown*).

Effect of Hydrophobic Inclusion Complex Formation of RE Molecules with TA-β-CD on Anthocyanin Release from PLA Implants

Preparation and Characterization of RE:TA-β-CD IC. Examination of *in vitro* release and polymer water uptake (see Figs. 5 and 7) and inner morphology (see Figs. 6 and 8) of 5 or 10 wt% RE-loaded PLGA 50:50, PLGA 85:15, and PLA implants indicated a difficulty to control the release of CS, CG, and CR from the implants due to high polymer water uptake and porosity. Among the four commonly found anthocyanins in RE, we identified three anthocyanins in the encapsulated RE, and their total content (CS + CG + CR) was determined to be 5.3 wt%. The remaining very large non-anthocyanin fraction of RE is known to contain other vital components, including phenolics (ellagic, ferulic, and *p*-coumeric acid), vitamins (ascorbic acid, α and β-carotene and folate), and minerals (12,13,32). The results of initial formulations studied above and high water solubility of non-anthocyanin fraction components (12,13,32,33) suggested the necessity of reducing the rapid release of non-anthocyanin fraction molecules from the implants to obtain an optimum sustained release of anthocyanin fraction molecules. Nevertheless, it is also advantageous to sustain the release of non-anthocyanin fraction molecules from the implants, as these components are shown to influence the chemopreventive

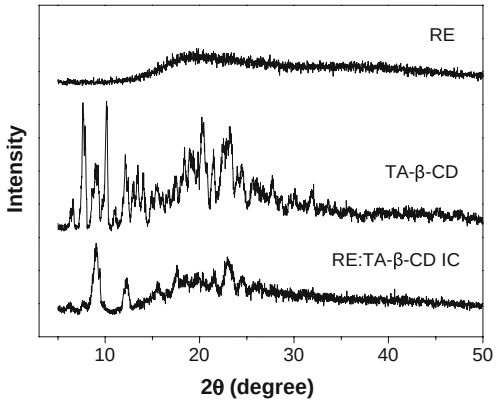

Fig. 9. X-ray diffraction of the formation of an inclusion complex of RE molecules with triacetyl-β-cyclodextrin (TA-β-CD) (RE:TA-β-CD IC).

potential of anthocyanins in oral SSC (12,13). Thus, to reduce the rapid release of non-anthocyanin fraction molecules (and hence the polymer water uptake and porosity), we formed the hydrophobic inclusion complex of RE molecules with TA-β-CD. TA-β-CD is a hydrophobic derivative of β-cyclodextrin (practically insoluble in water) and has proven to be a potential hydrophobic inclusion complex-forming carrier to obtain sustained release of highly-water soluble molecules (34,35).

RE:TA-β-CD IC was prepared by kneading method at 1:1 mass ratio. The formation of the IC was studied by XRD and NMR. The X-ray diffraction pattern of RE, TA-β-CD, and RE:TA-β-CD IC is shown in Fig. 9. RE exhibited a hollow XRD pattern, indicating the presence of amorphous compounds in the extract. By contrast, TA-β-CD exhibited numerous sharp diffraction peaks, particularly at 2θ of 7.6, 7.9, 10.1, 12.1, 20.2, and 23.1°, indicating the crystalline character of TA-β-CD. Compared to the RE and TA-β-CD XRD patterns, the XRD pattern of RE:TA-β-CD IC was reasonably different. For RE:TA-β-CD IC, the major diffraction peaks of TA-β-CD, observed at 2θ of 7.6, 10.1, and 20.2° were shifted to 2θ of 9.1, 12.3, and 23.0°, respectively. In addition, the intensity of all the major diffraction peaks of TA-β-CD was significantly reduced in the XRD pattern of RE:TA-β-CD IC. Shifts in 2θ value, reduction in intensity and disappearance of some diffraction peaks of TA-β-CD are indicative of formation of inclusion complex with RE molecules, as the change in crystallinity of cyclodextrin arises due to interaction with other molecules (36–38).

To characterize RE:TA-β-CD IC further, ^{1}H NMR spectra of RE, TA-β-CD, and RE:TA-β-CD IC were obtained, and ^{1}H chemical shifts corresponding to RE's molecules and TA-β-CD were calculated. The induced chemical shift (Δδ) is the difference in chemical shifts in the presence and absence of the other reactants ($\Delta\delta = \delta_{(complex)} - \delta_{(free)}$). The induced shift can be either downfield (positive sign) or upfield (negative sign). A chemical shift variation of specific host or guest nucleus provides direct evidence for the formation of inclusion complexes (39–42). ^{1}H NMR spectra of RE, TA-β-CD, and RE:TA-β-CD IC are shown in Fig. 10. The protons of RE molecules (H-1 to H-11) and TA-β-CD (H-1 to H-7) involved in chemical shift (Δδ) are numbered as 1–11 or 1–7 in Fig. 10.

The ^{1}H-chemical shifts of the RE sample in both the free and the complexed state are reported in Table IV. As shown, the larger downfield shift (Δδ = + 0.035 to + 0.188) experienced by RE protons (H-1 to H-11) indicates strong hydrophobic interactions with TA-β-CD. Upon inclusion complex formation, the cause for significant downfield shift effect by guest protons has been attributed to a dielectric

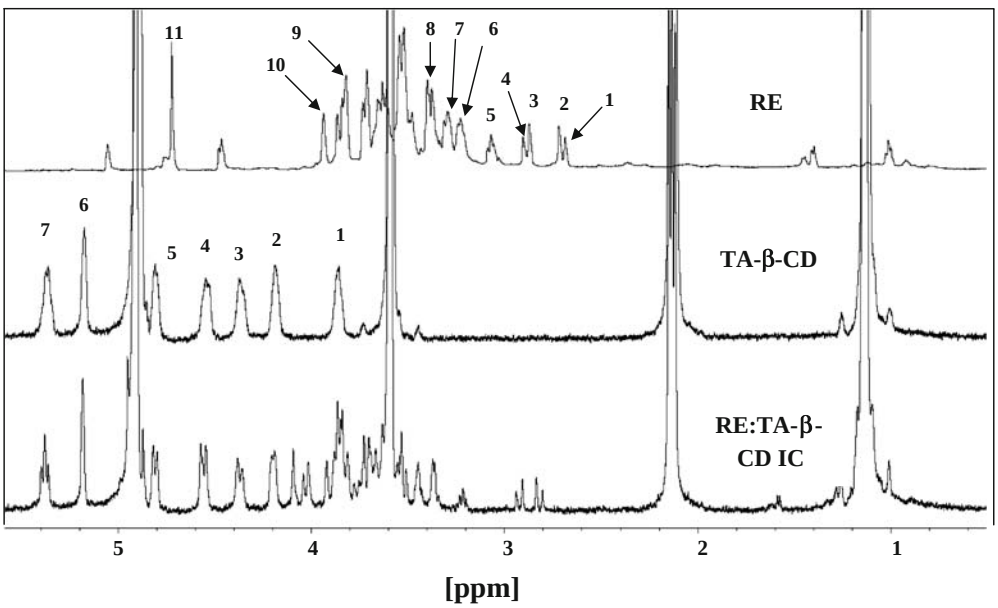

Fig. 10. Analysis of the inclusion complex formation of RE molecules with triacetyl-β-cyclodextrin (TA-β-CD) (RE:TA-β-CD IC) by NMR. Examination of change in the chemical shift of RE molecules or TA-β-CD in the presence and absence of TA-β-CD and RE. ^{1}H NMR spectra is shown for RE, TA-β-CD, and RE:TA-β-CD IC. The NMR samples, concentration was 1 mg/mL in 1.5% (*v*/*v*) D_3PO_4 (RE) and 80/20 (*v*/*v*) CD_3CD_2OD/1.5% (*v*/*v*) D_3PO_4 (TA-β-CD and RE:TA-β-CD IC).

Table IV. Chemical Shifts Corresponding to RE Molecules and Triacetyl-β-Cyclodextrin (TA-β-CD) in the Presence and Absence of TA-β-CD and RE Molecules

Protons	$\delta_{(free)}$	$\delta_{(complex)}$	$\Delta\delta^a$
RE's molecules			
H-1	2.685	2.802	+0.117
H-2	2.716	2.833	+0.117
H-3	2.870	2.905	+0.035
H-4	2.901	2.937	+0.036
H-5	3.059	3.214	+0.115
H-6	3.227	3.360	+0.133
H-7	3.290	3.423	+0.133
H-8	3.376	3.507	+0.131
H-9	3.837	4.025	+0.188
H-10	3.936	4.093	+0.157
H-11	4.759	4.817	+0.058
TA-β-CD			
H-1	3.857	3.847	−0.010
H-2	4.188	4.190	+0.002
H-3	4.374	4.367	−0.007
H-4	4.546	4.543	−0.003
H-5	4.808	4.797	−0.011
H-6	5.116	5.183	+0.067
H-7	5.367	5.358	−0.009
$-COCH_3$	2.143	2.138	−0.005

[a] $\Delta\delta = \delta_{(complex)} - \delta_{(free)}$

change in proton's surrounding environment imposed by inclusion inside the hydrophobic cavity (39). To study further, in the presence and absence of RE molecules, we also obtained the induced chemical shift (Δδ) for TA-β-CD protons (see Table IV). Not surprisingly, in the presence of RE molecules, TA-β-CD protons, particularly the cyclodextrin cavity (interior) protons (H-3 and H-7) (39,41–43), exhibited an upfield shift (Δδ = −0.007 and −0.009, respectively). The upfield shift induced by cyclodextrin protons can be attributed to magnetic anisotropic effects

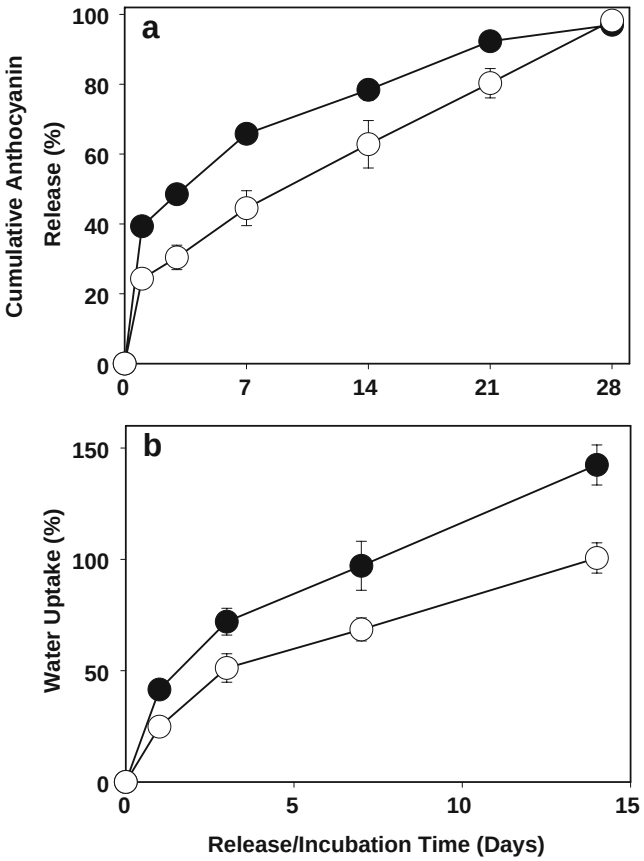

Fig. 12. Effect of formation of hydrophobic inclusion complex (IC) of RE molecules with triacetyl-β-cyclodextrin (TA-β-CD) on cumulative anthocyanin (sum of CG and CR) release (**a**) and polymer water uptake (**b**) characteristics of millicylindrical PLA (i.v. = 0.58 dl/g) implants. Cumulative anthocyanin release and polymer water uptake characteristics of 10 wt% (theoretical) RE (*filled circle*) and 20 wt% (theoretical) RE:TA-β-CD IC (*open circle*)-loaded PLA implants. Studies were carried out in PBST (pH 7.4) at 37°C and symbols represent mean ± SE, n=3.

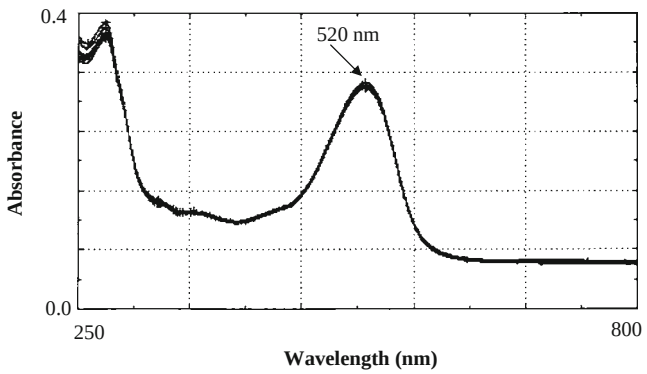

Fig. 11. Evaluation of the interaction of FBR anthocyanins with triacetyl-β-cyclodextrin (TA-β-CD). The UV-visible spectrum of 0.1 mg/mL RE in the absence and presence of TA-β-CD (0, 1, 2, 4, 8, and 9 mg/mL). RE or RE/TA-β-CD solutions were prepared in 80/20 ethanol/1.5% (*v*/*v*) phosphoric acid solution, and spectrum was obtained after 1 h of incubation at room temperature. The spectra of RE/TA-β-CD solutions were similar to RE solution, and hence naming of spectra could not be done distinctly.

exerted by the guest molecules (42). The downfield and upfield shifts exerted respectively by RE molecules and TA-β-CD protons indicate the formation of inclusion complex of RE molecules with TA-β-CD.

To understand specifically the interaction of identified anthocyanins (CS, CG, and CR) with TA-β-CD, we then employed UV-visible spectroscopy. Changes in the UV-visible absorption spectrum (shift in the absorption maxima or band) have been observed when a molecule forms inclusion complex with cyclodextrin derivatives (42,44). In the present study, the effect of TA-β-CD on the visible absorption band of anthocyanins was qualitatively investigated by keeping the concentration of the guest constant (RE concentration = 0.1 mg/mL) and by varying the host concentration between 1 to 9 mg/mL for TA-β-CD. The absorption band of anthocyanins at 520 nm did not change at varying concentration of TA-β-CD (see Fig. 11), suggesting the absence of interaction of anthocyanins with TA-β-CD. Based on the XRD, ^{1}H NMR and UV-visible spectroscopy results, it can be emphasized that not the anthocyanins but other unidentified hydrophilic and osmotically active molecules (non-anthocyanin fraction

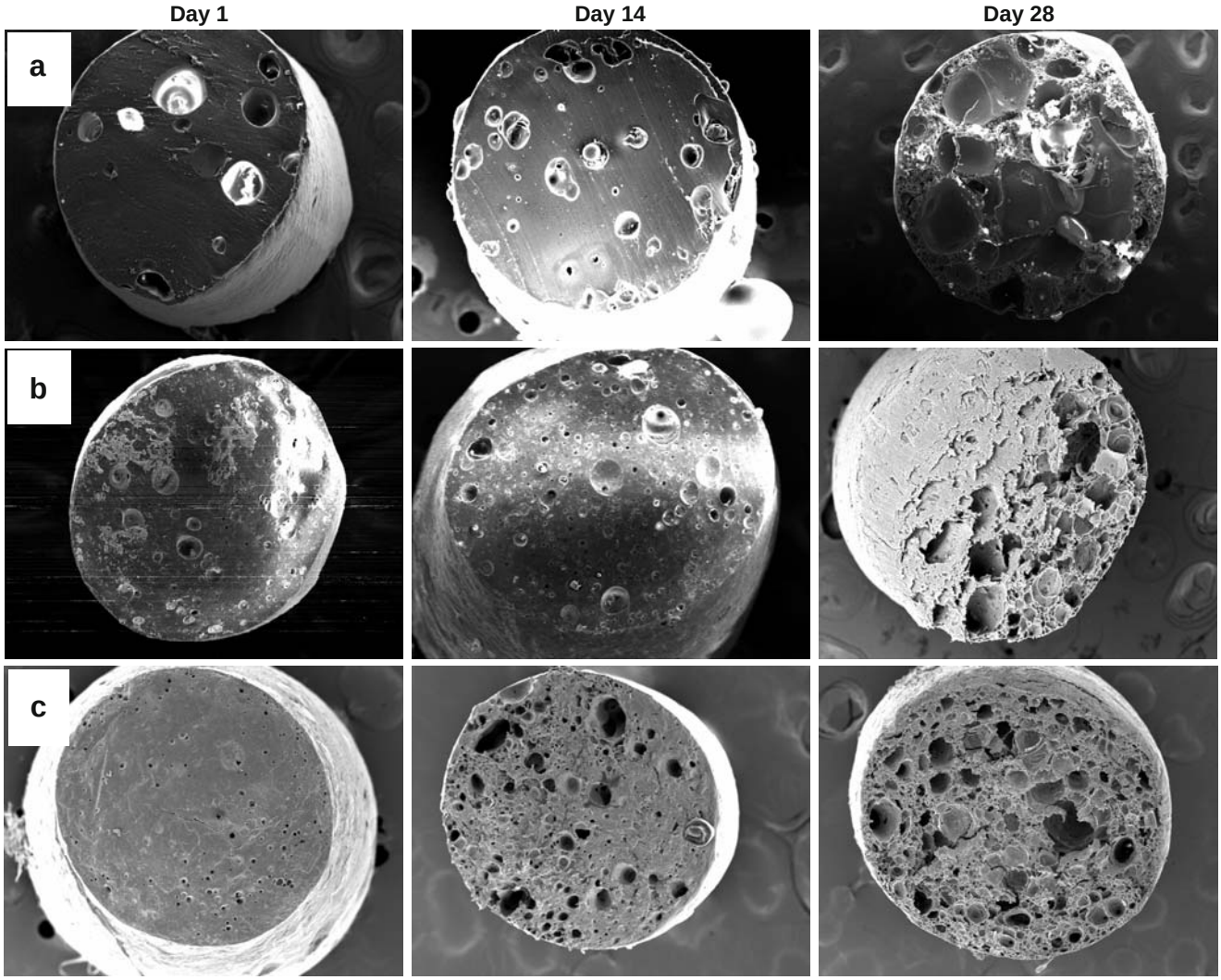

Fig. 13. Effect of formation of hydrophobic inclusion complex (IC) of RE molecules with triacetyl-β-cyclodextrin (TA-β-CD) on inner morphology of PLA (i.v. = 0.58 dl/g) millicylindrical implants after 1, 14 and 28 days of immersion in PBST at 37°C (**a** and **b**) or subcutaneous implantation in male Sprague-Dawley rats (**c**). SEM images are displayed for 10 wt% (theoretical) RE (**a**) and 20 wt% (theoretical) RE:TA-β-CD IC (**b** and **c**)-loaded PLA millicylindrical implants.

molecules) of the RE are involved in the formation of IC with TA-β-CD.

Effect on In-Vitro Anthocyanin Release from PLA Implants. The effect of formation of hydrophobic IC of RE molecules with TA-β-CD on *in vitro* anthocyanin (sum of CG and CR) release and polymer water uptake characteristics of millicylindrical PLA implants is shown in Fig. 12. Formation of hydrophobic IC not only reduced the initial burst considerably, but also provided better prolonged release of FBR anthocyanins from implants (see Fig. 12a), indicating the slow release of RE (anthocyanin and non-anthocyanin fraction) molecules from the IC-loaded implants. Consistent with these results, lower polymer water uptake (see Fig. 12b) and less polymer porosity (see Fig. 13) were exhibited by the 20 wt% IC-loaded PLA implants than by the 10 wt% RE/PLA implants, thereby providing slow and continuous release of anthocyanins from IC/PLA implants over a period of 28 days. In addition, the difference in release between individual anthocyanins (CS, CG and CR), which was not affected by RE loading and lactide content of the polymer, was also noticeably affected by the formation of hydrophobic IC (*data not shown*).

In Vivo Anthocyanin Release and In Vitro-In-Vivo Anthocyanin Release Correlation Characteristics of RE:TA-β-CD IC/PLA Millicylindrical Implants. Among the PLGA and PLA millicylindrical implant formulations tested *in vitro* for achieving slow and continuous anthocyanin release, 20 wt% RE:TA-β-CD IC/PLA implants exhibited better controlled release behavior. To evaluate the efficacy of this formulation further, *in vivo* anthocyanin release from 20 wt% RE:TA-β-CD IC/PLA implants was conducted in male Sprague-Dawley rats (see Fig. 14). As shown in Fig. 14a, when administered *in vivo*, IC-loaded PLA implants also exhibited low initial burst effect (16% anthocyanin (sum of CG + CR) release after 1 day) and provided 1-month slow and continuous release of anthocyanins (CG + CR). Importantly, an *in vitro-in vivo* correlation (level A) of anthocyanin release from IC-loaded PLA implants was performed (*in vitro vs. in vivo* release plot (*data not shown*)),

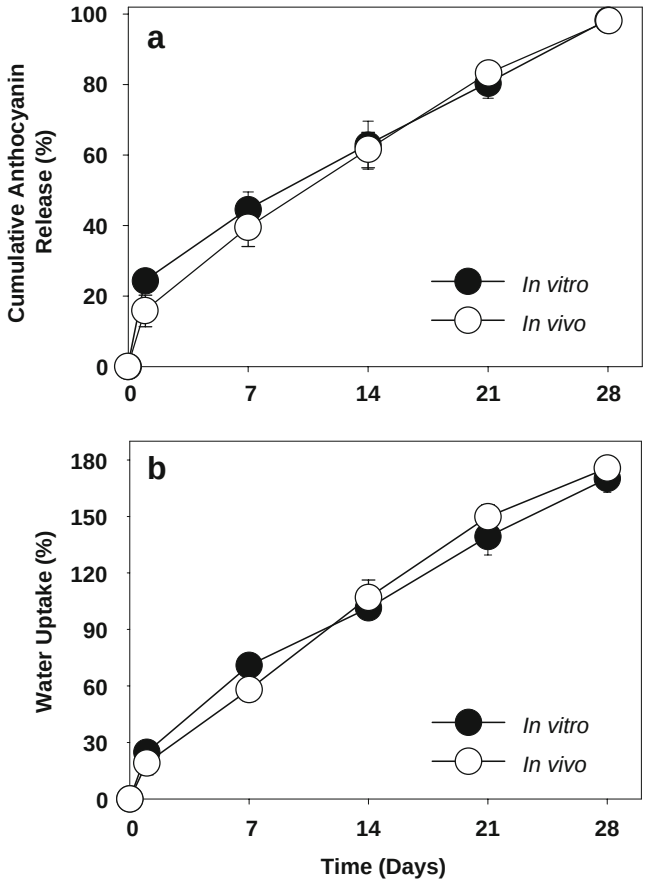

Fig. 14. Comparison of *in vitro and in vivo* cumulative anthocyanin (sum of CG and CR) release (**a**) and polymer water uptake (**b**) characteristics of 20 wt% (theoretical) RE:TA-β-CD IC-loaded millicylindrical PLA (i.v. = 0.58 dl/g) implants. Studies were carried out in PBST (pH 7.4) at 37°C (*in vitro*) or after subcutaneous administration in male Sprague-Dawley rats (*in vivo*) and symbols represent mean ± SE, n=3 (*in vitro*) or 5 (*in vivo*). *In vitro* data are replotted from Fig. 12 for comparison. At each time point, there was no significant difference between *in vitro* and *in vivo* anthocyanin release and polymer water uptake ($P>0.05$).

and an excellent correlation (R^2=0.996) was observed. The data at each time point was further analyzed by two-tailed unpaired Student's *t*-test, and there was no significant difference ($P>0.05$) between *in vitro* and *in vivo* anthocyanin release from IC-loaded PLA implants. Consistent with this finding, *in vivo* polymer water uptake (see Fig. 14b) and porosity (see Fig 13) of IC-loaded implants were also very similar with *in vitro* results (excellent correlation (R^2=0.99) and no significant difference ($P>0.05$) between *in vitro-in vivo polymer water uptake*). These data further support the potential efficacy of IC-loaded PLA implants in providing 1-month slow and continuous delivery of chemopreventive anthocyanins.

In Vitro-In Vivo Chemical Stability of FBR Anthocyanins in PLGA/ PLA Polymers

The formation of degradation products of FBR anthocyanins in the PLGA and PLA polymers was examined by analyzing the chromatograms of polymer samples from *in vitro-in vivo* release study at different time points. Using the retention time of degradation products of reference compounds (see previous section) and by the co-elution technique (co-injection of completely degraded reference compounds + RE solutions), we then identified and monitored the degradation peaks of CS, CG, and CR molecules in RE or RE:TA-β-CD IC-loaded implants. The formation of degradation products of anthocyanins in the PLGA/PLA polymers was negligible, as the peak area of the degradation product was 2–5% of the stable anthocyanin peak (*data not shown*). Note that anthocyanin (CR) exhibited slow and lowest degradation profile (~ 80% remaining after 28 days) in a very acidic (pH = 2.4) medium (see Fig. 4b). Since the microclimate (μ) pH of these polymers was also found to be very acidic ($2.8 < \mu pH < 5.6$) (45,46), it is likely that the acidic polymer microclimate acted as a suitable environment for unreleased anthocyanins to remain stable, similar to PLGA stabilization of the lactone form of camptothecins (47,48).

CONCLUSIONS

The goal of this study was to characterize the FBR anthocyanins in RE and to formulate and characterize RE-encapsulated millicylindrical injectable implants for slow and continuous delivery of the anthocyanins. CS, CG, and CR were identified in encapsulated RE, and their respective content in RE was 0.23, 1.53, and 3.53 wt%. PLGA/PLA implants loaded with 5 or 10 wt% RE exhibited high initial burst and short release duration of anthocyanins. High initial burst and short release duration of anthocyanins from PLGA/PLA implants was attributed to high polymer water uptake and porosity caused by very hydrophilic components of large non-anthocyanin fraction of RE. Formation of hydrophobic IC of non-anthocyanin fraction molecules with TA-β-CD provided optimal *in vitro/in vivo* initial burst effect and 1-month slow and continuous release of chemopreventive anthocyanins (CS, CG and CR).

ACKNOWLEDGEMENT

This study was supported by NIH R01 CA95901 and NIH R01 CA129609. We thank Dr. Scott Woehler, College of Pharmacy, University of Michigan, for the technical assistance with the NMR analysis.

REFERENCES

1. Jemal A, Siegel R, Ward E, Hao YP, Xu JQ, Murray T, *et al.* Cancer statistics. CA-Cancer J Clin. 2008;58:71–96.
2. Braakhuis BJM, Tabor MP, Leemans CR, van der Waal I, Snow GB, Brakenhoff RH. Second primary tumors and field cancerization in oral and oropharyngeal cancer: molecular techniques provide new insights and definitions. Head Neck-J Sci Spec. 2002;24:198–206.
3. Malone JP, Stephens JA, Grecula JC, Rhoades CA, Ba BAG, Ghaheri BA, *et al.* Disease control, survival, and functional outcome after multimodal treatment for advanced-stage tongue base cancer. Head Neck-J Sci Spec. 2004;26:561–72.

4. Pathak KA, Gupta S, Talole S, Khanna V, Chaturvedi P, Deshpande MS, *et al.* Advanced squamous cell carcinoma of lower gingivobuccal complex: patterns of spread and failure. Head Neck-J Sci Spec. 2005;27:597–602.
5. Desai KGH, Mallery SR, Schwendeman SP. Formulation and characterization of injectable poly(DL-lactide-co-glycolide) implants loaded with N-acetylcysteine, a MMP inhibitor. Pharm Res. 2008;25:586–97.
6. Mallery SR, Zwick JC, Pei P, Tong M, Larsen PE, Shumway BS, *et al.* Topical application of a bioadhesive black raspberry gel modulates gene expression and reduces cyclooxygenase 2 protein in human premalignant oral lesions. Cancer Res. 2008;68:4945–57.
7. Rodrigo KA, Rawal Y, Renner RJ, Schwartz SJ, Tian QG, Larsen PE, *et al.* Suppression of the tumorigenic phenotype in human oral squamous cell carcinoma cells by an ethanol extract derived from freeze-dried black raspberries, *Symposium on Berries in Cancer Prevention*. Lahti: Lawrence Erlbaum Assoc Inc; 2004. p. 58–68.
8. Rodrigo KA, Rawal Y, Renner RJ, Schwartz SJ, Tian QG, Larsen PE, *et al.* Suppression of the tumorigenic phenotype in human oral squamous cell carcinoma cells by an ethanol extract derived from freeze-dried black raspberries. Nutr Cancer. 2006;54:58–68.
9. Shumway BS, Kresty LA, Larsen PE, Zwick JC, Lu B, Field HW, *et al.* Effects of a topically applied bioadhesive berry gel on loss of heterozygosity indices in premalignant oral lesions. Clin Cancer Res. 2008;14:2421–30.
10. Ugalde CM, Liu ZF, Ren C, Chan KK, Rodrigo KA, Ling Y, *et al.* Distribution of anthocyanins delivered from a bioadhesive black raspberry gel following topical intraoral application in normal healthy volunteers. Pharm Res. 2009;26:977–86.
11. Tian QG, Giusti MM, Stoner GD, Schwartz SJ. Screening for anthocyanins using high-performance liquid chromatography coupled to electrospray ionization tandem mass spectrometry with precursor-ion analysis, product-ion analysis, common-neutral-loss analysis, and selected reaction monitoring. J Chromatogr A. 2005;1091:72–82.
12. Kresty LA, Morse MA, Morgan C, Carlton PS, Lu J, Gupta A, *et al.* Chemoprevention of esophageal tumorigenesis by dietary administration of lyophilized black raspberries. Cancer Res. 2001;61:6112–9.
13. Mallery SR, Stoner GD, Larsen PE, Fields HW, Rodrigo KA, Schwartz SJ, *et al.* Formulation and *in-vitro* and *in-vivo* evaluation of a mucoadhesive gel containing freeze dried black raspberries: implications for oral cancer chemoprevention. Pharm Res. 2007;24:728–37.
14. Stoner GD, Sardo C, Apseloff G, Mullet D, Wargo W, Pound V, *et al.* Pharmacokinetics of anthocyanins and ellagic acid in healthy volunteers fed freeze-dried black raspberries daily for 7 days. J Clin Pharmacol. 2005;45:1153–64.
15. Tian QG, Giusti MM, Stoner GD, Schwartz SJ. Urinary excretion of black raspberry (Rubus occidentalis) anthocyanins and their metabolites. J Agric Food Chem. 2006;54: 1467–72.
16. Hecht SS, Huang CS, Stoner GD, Li JX, Kenney PMJ, Sturla SJ, *et al.* Identification of cyanidin glycosides as constituents of freeze-dried black raspberries which inhibit anti-benzo[a]pyrene-7, 8-diol-9, 10-epoxide induced NF kappa B and AP-1 activity. Carcinogenesis. 2006;27:1617–26.
17. Huang CS, Li JX, Song L, Zhang DY, Tong QS, Ding M, *et al.* Black raspberry extracts inhibit benzo(a)pyrene Diol-epoxide-induced activator protein 1 activation and VEGF transcription by targeting the phosphotidylinositol 3-Kinase/Akt pathway. Cancer Res. 2006;66:581–7.
18. Wang LS, Hecht SS, Carmella SG, Yu NX, Larue B, Henry C, *et al.* Anthocyanins in black raspberries prevent esophageal tumors in rats. Cancer Prev Res. 2009;2:84–93.
19. Mallery SR, Pei P, Kang JC, Ness GM, Ortiz R, Touhalisky JE, *et al.* Controlled-release of doxorubicin from poly(lactide-co-glycolide) microspheres significantly enhances cytotoxicity against cultured AIDS-related kaposi's sarcoma cells. Anticancer Res. 2000;20:2817–25.
20. Weinberg BD, Ai H, Blanco E, Anderson JM, Gao JM. Antitumor efficacy and local distribution of doxorubicin via intratumoral delivery from polymer millirods. J Biomed Mater Res A. 2007;81A:161–70.
21. Weinberg BD, Blanco E, Lempka SF, Anderson JM, Exner AA, Gao JM. Combined radiofrequency ablation and doxorubicin-eluting polymer implants for liver cancer treatment. J Biomed Mater Res A. 2007;81A:205–13.
22. Mullen W, Lean MEJ, Crozier A. Rapid characterization of anthocyanins in red raspberry fruit by high-performance liquid chromatography coupled to single quadrupole mass spectrometry. J Chromatogr A. 2002;966:63–70.
23. Tian QG, Giusti MM, Stoner GD, Schwartz SJ. Characterization of a new anthocyanin in black raspberries (Rubus occidentalis) by liquid chromatography electrospray ionization tandem mass spectrometry. Food Chem. 2006;94:465–8.
24. Wu XL, Prior RL. Systematic identification and characterization of anthocyanins by HPLC-ESI-MS/MS in common foods in the United States: fruits and berries. J Agric Food Chem. 2005;53: 2589–99.
25. Kirca A, Ozkan M, Cemeroglu B. Effects of temperature, solid content and pH on the stability of black carrot anthocyanins. Food Chem. 2007;101:212–8.
26. Hubbermann EM, Heins A, Stockmann H, Schwarz K. Influence of acids, salt, sugars and hydrocolloids on the colour stability of anthocyanin rich black currant and elderberry concentrates. Eur Food Res Technol. 2006;223:83–90.
27. Xiong SY, Melton LD, Easteal AJ, Siew D. Stability and antioxidant activity of black currant anthocyanins in solution and encapsulated in glucan gel. J Agric Food Chem. 2006;54: 6201–8.
28. Kong JM, Chia LS, Goh NK, Chia TF, Brouillard R. Analysis and biological activities of anthocyanins. Phytochemistry. 2003;64:923–33.
29. Knobloch TJ, Casto BC, Kresty LA, Stoner GD, D'Ambrosio SM, Mallery SR, *et al.* Bench to bedside: chemoprevention of oral cancer by black raspberries. Cancer Epidem Biomar. 2005;14:2751S–2.
30. Casto BC, Kresty LA, Kraly CL, Pearl DK, Knobloch TJ, Schut HA, *et al.* Chemoprevention of oral cancer by black raspberries. Anticancer Res. 2002;22:4005–15.
31. Blanco E, Weinberg BD, Stowe NT, Anderson JM, Gao JM. Local release of dexamethasone from polymer millirods effectively prevents fibrosis after radiofrequency ablation. J Biomed Mater Res A. 2006;76:174–82.
32. Shahidi F, Naczk M. Phenolics in food and nutraceuticals. Boca Raton: CRC; 2004.
33. Dai J, Gupte A, Gates L, Mumper RJ. A comprehensive study of anthocyanin-containing extracts from selected blackberry cultivars: extraction methods, stability, anticancer properties and mechanisms. Food Chem Toxicol. 2009;47:837–47.
34. Fernandes CM, Ramos P, Falcao AC, Veiga FJB. Hydrophilic and hydrophobic cyclodextrins in a new sustained release oral formulation of nicardipine: *in vitro* evaluation and bioavailability studies in rabbits. J Controlled Release. 2003;88:127–34.
35. Ikeda Y, Kimura K, Hirayama F, Arima H, Uekama K. Controlled release of a water-soluble drug, captopril, by a combination of hydrophilic and hydrophobic cyclodextrin derivatives. J Controlled Release. 2000;66:271–80.
36. Fischer W, Klokkers K. Crystalline cyclodextrin complexes of ranitidine hydrochloride, process for their preparation and pharmaceutical compositions containing the same. US *Patent:5,665,767*; 1997.
37. Rao KR, Bhanumathi N, Yadav JS, Krishnaveni NS. Inclusion complex of rifampicin, an anti-tubercular drug, with β-cyclodextrin or 2-hydroxypropyl-β-cyclodextrin and a process thereof. US *Patent:7,001,893*; 2006.
38. Huh KM, Ooya T, Sasaki S, Yui N. Polymer inclusion complex consisting of poly(epsilon-lysine) and α-cyclodextrin. Macromolecules. 2001;34:2402–4.
39. Amato ME, Lipkowitz KB, Lombardo GM, Pappalardo GC. High-field NMR spectroscopic techniques combined with molecular dynamics simulations for the study of the inclusion complexes of α- and β-cyclodextrins with the cognition activator 3-phenoxypyridine sulphate (CI-844). Magn Reson Chem. 1998;36:693–705.
40. Beni S, Szakacs Z, Csernak O, Barcza L, Noszal B. Cyclodextrin/imatinib complexation: binding mode and charge dependent stabilities. Eur J Pharm Sci. 2007;30:167–74.

41. Fernandes CM, Carvalho RA, da Costa SP, Veiga FJB. Multimodal molecular encapsulation of nicardipine hydrochloride by β-cyclodextrin, hydroxypropyl-β-cyclodextrin and triacetyl-β-cyclodextrin in solution. Structural studies by ^{1}H NMR and ROESY experiments. Eur J Pharm Sci. 2003;18:285–96.
42. Ramusino MC, Bartolomei M, Gallinella B. ^{1}H NMR, UV and circular dichroism study of inclusion complex formation between the 5-lipoxygenase inhibitor zileuton and β- and γ-cyclodextrins. J Inclus Phenom Mol. 1998;32:485–98.
43. Djedaini F, Lin SZ, Perly B, Wouessidjewe D. High-field nuclear-magnetic-resonance techniques for the investigation of a β-cyclodextrin-indomethacin inclusion complex. J Pharm Sci. 1990;79:643–6.
44. Ma DQ, Rajewski RA, Vander Velde D, Stella VJ. Comparative effects of (SBE)(7 m)-beta-CD and HP-beta-CD on the stability of two anti-neoplastic agents, melphalan and carmustine. J Pharm Sci. 2000;89:275–87.
45. Ding AG, Schwendeman SP. Acidic microclimate pH distribution in PLGA microspheres monitored by confocal laser scanning microscopy. Pharm Res. 2008;25:2041–52.
46. Ding AG, Shenderova A, Schwendeman SP. Prediction of microclimate pH in poly(lactic-co-glycolic acid) films. J Am Chem Soc. 2006;128:5384–90.
47. Shenderova A, Burke TG, Schwendeman SP. Stabilization of 10-hydroxycamptothecin in poly(lactide-co-glycolide) microsphere delivery vehicles. Pharm Res. 1997;14:1406–14.
48. Shenderova A, Burke TG, Schwendeman SP. The acidic microclimate in poly(lactide-co-glycolide) microspheres stabilizes camptothecins. Pharm Res. 1999;16:241–8.